

ARTICLE

Received 16 Sep 2016 | Accepted 16 May 2017 | Published 21 Jul 2017

DOI: 10.1038/ncomms15977

OPEN

Nrp2 is sufficient to instruct circuit formation of mitral-cells to mediate odour-induced attractive social responses

Kasumi Inokuchi^{1,2}, Fumiaki Imamura³, Haruki Takeuchi¹, Ryang Kim⁴, Hiroyuki Okuno⁴, Hirofumi Nishizumi^{1,2}, Haruhiko Bito⁴, Takefumi Kikusui⁵ & Hitoshi Sakano¹

Odour information induces various innate responses that are critical to the survival of the individual and for the species. An axon guidance molecule, Neuropilin 2 (Nrp2), is known to mediate targeting of olfactory sensory neurons (primary neurons), to the posteroventral main olfactory bulb (PV MOB) in mice. Here we report that Nrp2-positive (Nrp2⁺) mitral cells (MCs, second-order neurons) play crucial roles in transmitting attractive social signals from the PV MOB to the anterior part of medial amygdala (MeA). Semaphorin 3F, a repulsive ligand to Nrp2, regulates both migration of Nrp2⁺ MCs to the PV MOB and their axonal projection to the anterior MeA. In the MC-specific Nrp2 knockout mice, circuit formation of Nrp2⁺ MCs and odour-induced attractive social responses are impaired. *In utero*, electroporation demonstrates that activation of the *Nrp2* gene in MCs is sufficient to instruct their circuit formation from the PV MOB to the anterior MeA.

¹Department of Brain Function, School of Medical Science, University of Fukui, Fukui 910-1193, Japan. ²Department of Biophysics and Biochemistry, Graduate School of Science, The University of Tokyo, Tokyo 113-0032, Japan. ³Department of Pharmacology, Pennsylvania State University College of Medicine, Hershey, Pennsylvania 17033, USA. ⁴Department of Neurochemistry, Graduate School of Medicine, The University of Tokyo, Tokyo 113-0033, Japan. ⁵Department of Animal Science and Biotechnology, School of Veterinary Medicine, Azabu University, Sagamihara, Kanagawa 252-5201, Japan. Correspondence and requests for materials should be addressed to H.S. (email: sakano.hts@gmail.com).

The mammalian olfactory system recognizes a diverse repertoire of chemical information that induces distinct behavioural responses based on the odour qualities¹. In rodents, odour ligands are detected by odorant receptors (ORs) of olfactory sensory neurons (OSNs) in the olfactory epithelium (OE)². Since OSNs expressing the same type of OR send their axons to a specific target site, glomerulus, and each odorant can interact with multiple OR species^{3–5}, odour signals detected in the OE are converted into a topographic map of activated glomeruli. Odour information encoded in the olfactory bulb (OB) is then conveyed by projection neurons, mitral/tufted (M/T) cells, to various areas of the olfactory cortex (OC) to elicit odour responses^{6,7}. How is it then that the map information is transmitted from the OB to the OC for behavioural decisions? For olfactory map formation, OSN axons are guided to approximate locations in the OB by using different sets of axon guidance molecules^{8–11} and the map is further refined in an activity-dependent manner¹². In contrast to the primary projection of OSNs, molecular mechanisms for the circuit formation of M/T cells are largely unknown.

How is the odour map interpreted and how are odour qualities determined for behavioural decisions? The olfactory map is not merely a projection screen that recognizes patterns to discriminate various odorants, but it is composed of functional domains that induce innate odour responses¹³. We have previously reported that the avoidance domain for spoiled foods and the fear domain for predator odours are separately located in the dorsal part of the OB, in D_I and D_{II} regions, respectively¹⁴. The cortical amygdala (CoA) is reported to mediate odour information of aversive smells^{15,16}. As for the attractive social cues, responding glomeruli are found in the posteroventral (PV) part of the OB. For example, male urine compounds methylthio-methanethiol (MTMT)¹⁷ and (Z)-e-tetradecen-1-ol (5Z-14:OH)¹⁸ are detected by MOR83 and MOR286-3P, respectively, whose glomeruli are located in the PV OB¹⁹. Although neural circuits have not been established for these social cues, the medial amygdala (MeA) is reported to respond to odour inputs for attractive responses²⁰. We assume specific circuit links between functional domains in the OB and particular regions in the OC to induce behavioural outputs.

The MeA is known to elicit pheromone-induced innate behaviours by receiving signals from the accessory OB (AOB)^{16,20,21}. However, the MeA receives social odour signals also from the main OB (MOB). Dye-injection and pharmacological ablation experiments support this notion^{22,23}. Furthermore, some attraction behaviours mediated by the MeA are not affected in the knockout (KO) of TrpC2 (AOB-specific ion channel)^{24–26}, but impaired in the KO of CNG-A2 (MOB-specific ion channel)²⁷. Although these previous experiments indicate that the main olfactory system plays a critical role in inducing attractive social responses, the exact mechanism for how odour signals are correctly transmitted from the MOB to the MeA remains uncertain. It is also unclear whether the second-order neurons, M/T cells, can be divided into different subsets for specific roles and how their cell lineages are determined during development. Thus, it is quite important that the functional and structural connectivity between the MOB and the OC be elucidated.

Here we report that a subset of mitral cells (MCs) that are Neuropilin 2-positive (Nrp2⁺) play a critical role in transmitting attractive social signals from the PV MOB to the anterior MeA. In the MC-specific conditional KO (cKO) of Nrp2, both circuit formation of Nrp2⁺ MCs and odour-induced social attraction behaviours are impaired. Furthermore, *in utero*, electroporation demonstrates that activation of the *Nrp2* gene in MCs is sufficient to instruct circuit formation from the PV MOB to the anterior MeA.

Results

Nrp2⁺ MCs in the MOB elicit social attraction responses. We have previously reported that Nrp2⁺ OSN axons are guided from the ventral OE to the PV MOB by repulsive interactions with Semaphorin 3F (Sema3F) secreted by dorsal OSN axons¹¹. Furthermore, a subpopulation of MCs in the PV MOB are Nrp2⁺ (refs 11,28). These observations suggested an intriguing possibility that Nrp2⁺ MCs may be responsible for receiving attractive social signals from the Nrp2⁺ glomeruli and transmitting the signals to the anterior MeA. We, thus, examined whether odour-induced social behaviours are affected in the Nrp2 cKO. MC-specific cKO mice were generated by crossing the Nrp2-floxed mice²⁹ with the AP2ε (immature MC marker)-Cre as a driver^{30,31}. AP2ε has restricted expression in the OB and represents the earliest known marker for the developing OB^{30–32}. To demonstrate the tissue-specific activity of Cre, we crossed the AP2ε-Cre line to the ROSA-stop-lacZ mouse³⁰. Heavy X-gal staining was found in the MC layer in the OB (Supplementary Fig. 1a); however, OSNs in the OE were devoid of staining.

Since the PV MOB is reported to be activated by urinary volatiles^{23,33}, we evaluated the response of male mice to female urine that was physically separated from the male mice so that only volatile social cues could be detected (Fig. 1a, left). In the control experiment, the heterozygous littermate male was strongly attracted to the female urine, sniffing it for much longer period of time compared to that of another male. In the male cKO of Nrp2, no difference was observed in sniffing between the female and male urine (Fig. 1a, right). We also examined whether the MTMT-induced female behaviours¹⁷ are affected in our cKO of Nrp2. It was found that investigation times of female mice were significantly lowered in the cKO towards MTMT with castrated male urine (Fig. 1b). Interestingly, female cKO demonstrated increased attraction to the castrated male urine alone compared with controls, which may be explained by alterations of neural circuitries in the Nrp2 cKO. These results supported the idea that Nrp2⁺ MOB MCs are involved in eliciting social attraction behaviours. However, one could not exclude the possibility that some diffusible urine components might have been processed by the vomeronasal organ (VNO). We, therefore, studied male-mouse ultrasonic vocalization (USV)³⁴ that is regulated independently from the VNO²⁴. USV signals emitted by resident males were compared between the cKO and heterozygous littermates in the presence of a female intruder. It was found that USV by males towards females was diminished in the MC-specific cKO of Nrp2 (Fig. 1c,d and Supplementary Fig. 1b).

We next studied suckling behaviour of pups in the MC-specific cKO of Nrp2. It is known that in neonatal rabbits, nipple search is a stereotyped innate behaviour regulated by maternal odour substances and independent of the AOB³⁵. Since the VNO is not fully functional until postnatal day 10 (P10) in mice³⁶, it is unlikely that suckling behaviour of pups is regulated by the VNO, but instead by the main olfactory system. In the control pups (heterozygous littermates), ~90% were able to successfully find their mother's nipples within 4 min (Fig. 1e). In contrast, <20% of mutant pups were able to locate the nipples. However, this difference was not due to any defect in locomotive activities. We placed pups on their back and determined the time they spent to recover from this position (Supplementary Fig. 1c). In this reflex righting test, no difference was found between the cKO and control littermates.

We previously reported that innate fear responses induced by a fox odour, trimethylthiazoline (TMT), are mediated by the dorsal-region glomeruli in the MOB¹⁴. Furthermore, the CoA is known to receive aversive information of TMT^{15,16}. To determine

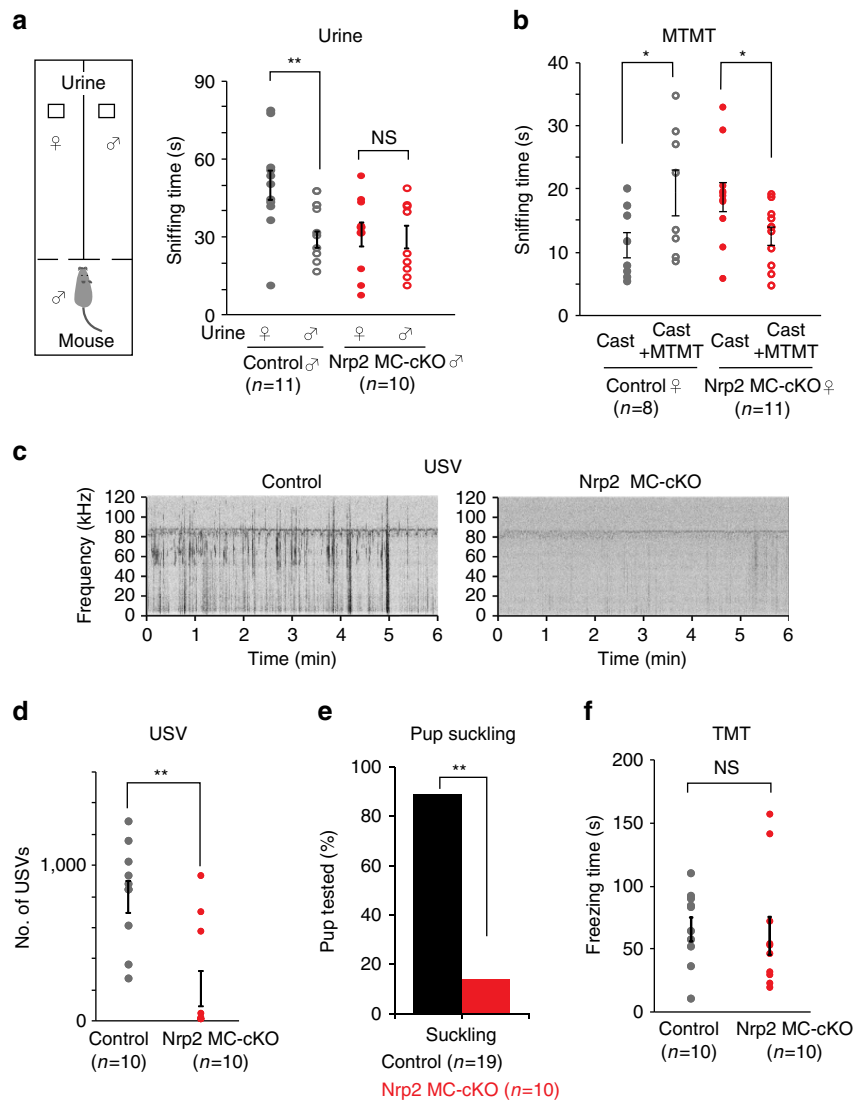


Figure 1 | Innate social behaviours in the MC-specific cKO of *Nrp2*. (a) The male attractive behaviour towards female urine. A piece of filter paper spotted with 60 μ l of male or female urine was presented to the male cKO or heterozygous littermate as a control. Sniffing time duration was measured within 5 min after presenting the filter paper. Although the control male spent longer times sniffing female urine, the cKO male did not show any preference. Data are presented in mean \pm s.e. $^{**}P < 0.01$, NS: not significant (Student's *t*-test). (b) The female attractive behaviour towards MTMT. A piece of filter paper spotted with 50 μ l of castrated male urine or castrated male urine with 20 p.p.b. MTMT was presented to the female cKO. Sniffing time duration was measured within 5 min after presenting the filter paper. Data are presented in mean \pm s.e. $^{*}P < 0.05$ (Student's *t*-test). (c) Spectrograms of USVs. USV signals emitted by resident males are compared between the cKO and heterozygous littermates in the presence of a female intruder. The intruder female was introduced into the cage for 6 min in each trial. Very few signals are detected in the cKO male. (d) Comparison of numbers of USV signals elicited by male mice in the presence of a WT female. USV is significantly reduced in the cKO. Data are presented in mean \pm s.e. $^{**}P < 0.05$ (Wilcoxon signed-rank test). (e) Suckling behaviour in the *Nrp2* MC-cKO pups. Lactating female mice were anaesthetized and laid sideways, exposing their nipples towards pups. Pups were fasted for 4 h before the experiment and placed \sim 1 cm away from the females' nipples. The time to find nipples for suckling was measured within 4 min. Most cKO pups failed to find nipples within 4 min. ($n = 19$ for the control, $n = 10$ for the MC-specific cKO of *Nrp2*). $^{**}P < 0.01$ (Z-test). (f) Fear responses to a predator's odour. A piece of filter paper spotted with 10 μ l of undiluted TMT was presented to the cKO and heterozygous littermate as a control. Freezing time lengths were measured during the 10 min exposure to TMT. NS: not significant (paired *t*-test). Data are presented in mean \pm s.e.

if *Nrp2*⁺ MCs are involved in eliciting fear responses to TMT, we examined TMT responsiveness in the MC-specific cKO of *Nrp2*. Interestingly, TMT-induced fear responses were not affected in the cKO (Fig. 1f). These observations demonstrate that the absence of *Nrp2* in MOB MCs interferes with social attraction behaviours, while having no effect on the TMT-induced innate fear responses that are mediated by the dorsal MOB. Furthermore, no abnormality was found in the detection of odour substances, such as α -terpinene and vanillin, that activate the dorsal glomeruli^{37,38}. No difference was found in the

habituation–dishabituation test between the cKO and heterozygous littermate mice (Supplementary Fig. 1d, left) even with the 10⁻⁵ dilution of vanillin for dishabituation (Supplementary Fig. 1d, right).

***Nrp2*⁺ MCs are guided to the PV MOB by Sema3F.** Having demonstrated that *Nrp2* is essential for critical social behaviours, such as USV communication, we could directly test the hypothesis that *Nrp2* is involved, and potentially instructive, in neural

circuit formation between the MOB and the anterior MeA. The significant changes in odour-induced social behaviours can be explained by the alterations in the neural circuitry in the *Nrp2* cKO. To examine this, we first analysed migration and distribution of *Nrp2*⁺ MCs in the MOB of the wild-type (WT) mice. In the embryo, MC precursors are generated in the ventricular zone at E10–13 and migrate radially, through the intermediate zone, to the mitral cell layer (MCL) in the MOB^{39,40} (Supplementary Fig. 2a). Double *in situ* hybridization, using *Pcdh21* (mature MC marker) and *Nrp2* probes, revealed that the *Nrp2* gene is expressed in a subset of MCs in the WT (Fig. 2a). *Nrp2* expression gradually decreases after birth and disappears by PD14. We, therefore, attempted to analyse how the two types of MCs, *Nrp2*⁺ and *Nrp2*⁻, are generated in the MOB during development. *Pcdh21* and *AP2ε* were used as developmental markers for mature and immature MCs, respectively. At E13.5, immature MCs (*AP2ε*⁺) are located within the intermediate zone, where the *Nrp2*⁺ and *Nrp2*⁻ cells are already separated (Supplementary Fig. 2b). *In situ* hybridization revealed that not all MCs in the PV MOB are *Nrp2*⁺ (Supplementary Fig. 2b). There may be another subset of MCs in the PV MOB, which is *Nrp2*⁻. It is possible that these *Nrp2*⁻ MCs were originally *Nrp2*⁺, but lost *Nrp2* expression after migrating to the PV. Our BrdU experiment indicates that both *Nrp2*⁺ and *Nrp2*⁻ MCs are simultaneously produced at E10–13 (Supplementary Fig. 2c). At P0, when most MCs have reached the MCL, *Nrp2*⁺ MCs are confined to the PV region of the MOB (Fig. 2a). As for the

primary neurons, dorsal OSN axons are *Nrp2*⁻, whereas the PV OSN axons are *Nrp2*⁺ (Fig. 2b)¹¹. Since MCs PV tend to extend their primary dendrites perpendicularly to the nearest glomerulus, *Nrp2*⁺ MC dendrites make synaptic connections with the *Nrp2*⁺ OSN axons in the PV MOB. This dorsal/ventral partitioning appears to provide a topographical and functional separation of the olfactory map^{11,14}.

To specifically examine how *Nrp2*⁺ MCs are guided to their proper locations in the MCL, and whether *Nrp2* regulates the association between OSN axons and MC dendrites, we analysed the *Nrp2* KO mouse²⁹. In this total KO, a coding sequence of *Nrp2* was replaced with that of *GFP*, so that cells with activated *Nrp2* promoter could be detected with the *GFP* probe. Our studies showed that not only the targeting of OSN axons (Fig. 3a, upper panel and Supplementary Fig. 3a), but also the distribution of MCs is affected in the KO mice (Fig. 3a, lower panel and Supplementary Fig. 3b). In contrast to the total KO, the MC-specific cKO of *Nrp2* did not affect the targeting of *Nrp2*⁺ OSN axons. Likewise, MC migration was not affected in the OSN-specific cKO of *Nrp2* (Fig. 3a and Supplementary Fig. 3b). On the basis of these observations, the possibility of direct crosstalk between the OSN axons and MC dendrites via *Nrp2* molecules was excluded. We, therefore, focused our attention on *Sema3F*, a repulsive ligand for *Nrp2*. *Sema3F* is secreted by the dorsal OSN axons to repel the ventral OSN axons and is not produced by MCs in the MOB¹¹. To examine whether the OSN-derived *Sema3F* also regulates the migration of MCs, we analysed the distribution of *Nrp2*⁺ MCs in the OSN-specific cKO of *Sema3F*. In this cKO, distribution of *Nrp2*⁺ MCs in the MOB is severely affected: *Nrp2*⁺ MCs are found not only in the ventral, but also in the dorsal part of the MCL (Fig. 3b, lower panel and Supplementary Fig. 3d). In the same *Sema3F* cKO, *Nrp2*⁺ OSN axons are also defasciculated in the glomerular layer (GL) (Fig. 3b, upper panel and Supplementary Fig. 3c). These phenotypes are similar to those observed in the total KO of either *Sema3F* or *Nrp2* (Fig. 3c,d). We performed these targeting experiments at both E18 and P0 and obtained basically the same results. However, signals were clearer at E18 than P0 in the hybridization experiment probably due to the differences in transcription levels of *Nrp2*. In contrast, we obtained better staining at P0 than E18 in the immunohistochemistry. Taken altogether, we conclude that for proper matching to occur, OSN-derived *Sema3F* in the dorsal MOB regulates both targeting of *Nrp2*⁺ OSN axons and migration of *Nrp2*⁺ MCs to the PV MOB.

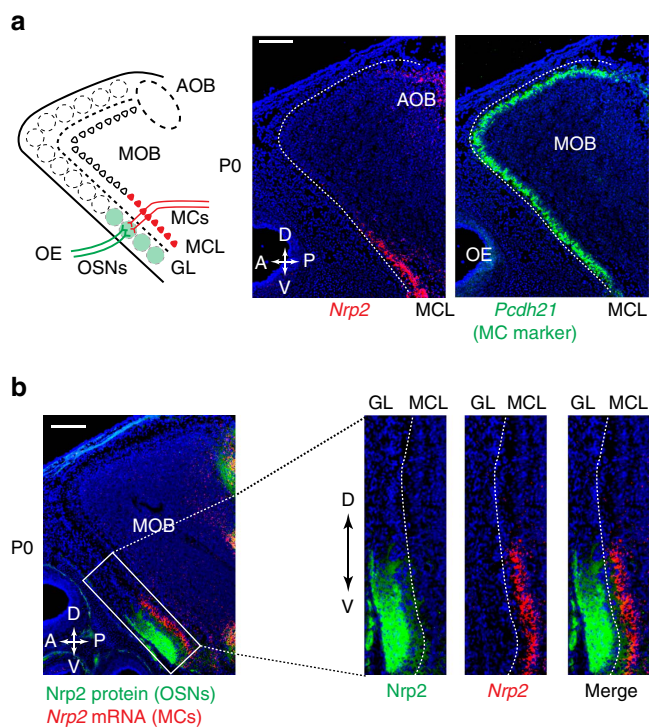
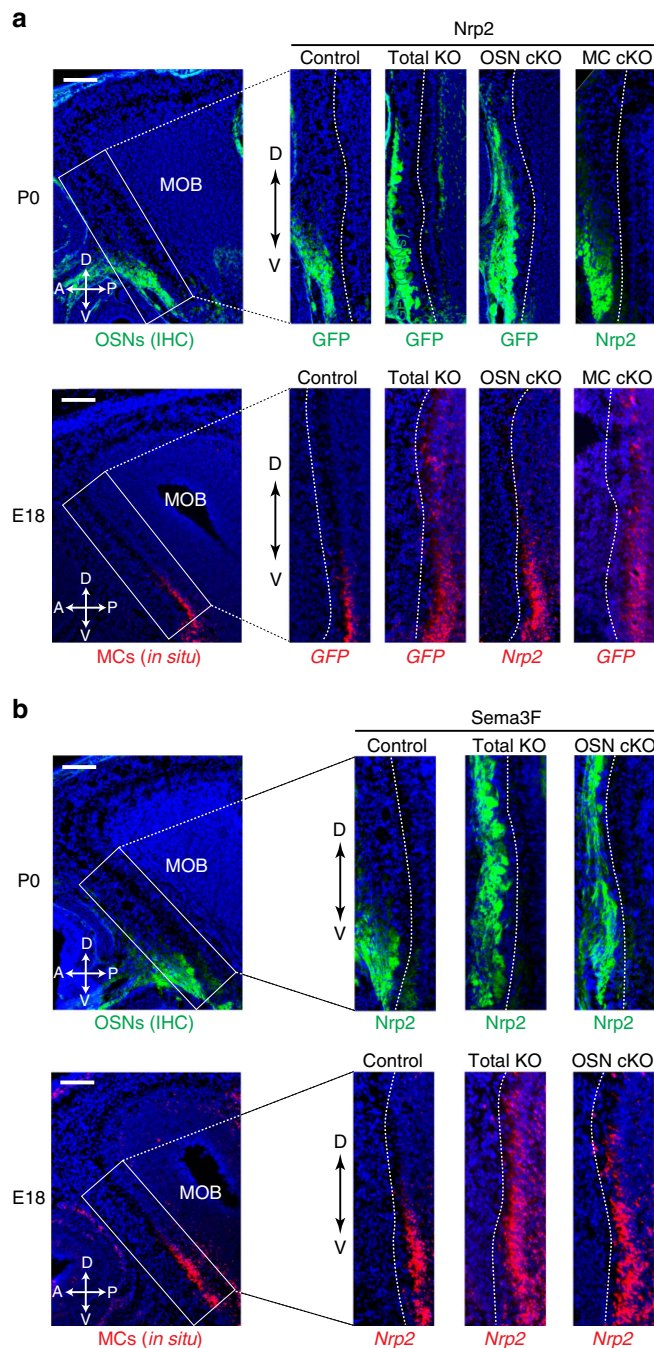


Figure 2 | Distribution of *Nrp2* in the GL and MCL of the MOB.

(a) Detection of *Nrp2* transcripts in the ventral-region MCs. Parasagittal MOB sections (P0) were hybridized with *Pcdh21* (MC marker) and *Nrp2* probes. $n = 5$. *Nrp2* is expressed in the MCL, high in the ventral and low in the dorsal region. *Nrp2*⁺ signals seen in the PD region represent *Nrp2*⁺ MCs in the AOB. A schematic diagram of the mouse MOB is shown in the left. (b) Distribution of *Nrp2* protein and *Nrp2* transcripts in the MOB. MOB sections at P0 were immunostained with anti-*Nrp2* antibodies or hybridized with the *Nrp2* probe. *Nrp2* and *Nrp2* signals are distributed in parallel along the D–V axis in the GL and MCL, respectively. Enlarged photos are shown in the right. $n = 5$. Scale bar, 200 μm .

***Nrp2*⁺ MCs target their axons to the anterior MeA.** To study a specific function of *Nrp2*⁺ MCs in inducing social attraction behaviours, we next analysed their axonal projection and arborization in the OC. MCs send their axons to various brain regions by following the lateral olfactory tract^{6,41–44} (Fig. 4a, right). Since *Nrp2* expression was not sufficiently strong for tracing axons by immunostaining, we developed a transgenic (Tg) mouse in which the fluorescent reporter protein, EYFP, was expressed in *Nrp2*⁺ MCs. To do this, we generated Tg mice carrying the transgene, *pcdh21-lacZ-STOP-tauEYFP*, in which the Cre-inducible *tauEYFP* gene was expressed with the *Pcdh21* promoter (Fig. 4a). The *lacZ* gene was introduced into the construct to monitor the *Pcdh21* promoter activity (Supplementary Fig. 4a, left). Four independent mouse lines, that successfully expressed the *lacZ* gene in MCs, were obtained. While the *Pcdh21* promoter is usually active in both the MOB and the AOB, in one of our four mouse lines, the transgene was activated only in the MOB and not in the AOB (Supplementary Fig. 4a, right). Signals of β -gal seen around the AOB are MC axons passing by from the MOB. This mouse line proved quite useful for analyzing MOB MCs for



axonal projection separately from AOB counterparts. To activate the *EYFP* gene specifically in the *Nrp2*⁺ MCs of the MOB, the mouse was then crossed with another Tg mouse containing the *Nrp2-Cre*, where Cre-recombinase was induced by the *Nrp2* promoter (Fig. 4a). As expected, EYFP signals were detected only in the PV-region MCs, but not in the dorsal ones (Supplementary Fig. 4b). This Tg mouse also allowed us to trace the trajectory of axonal projection of *Nrp2*⁺ MCs by immunostaining EYFP.

MCs in the MOB have been reported to project their axons to various regions of the OC, including the anterior olfactory nuclei (AON), piriform cortex (PIR) and CoA^{43,45–47}. Consistent with these previous reports, EYFP⁺ axons are found in the superficial layer of these nuclei (Fig. 4b, left). Staining signals of EYFP are uniformly distributed throughout these areas and no clustering of staining signals is observed. Interestingly, EYFP⁺ axons are

detected in the *Nos1*⁺ MeA (Supplementary Fig. 4c), but are negative for OCAM, a marker for dorsal-region MCs⁴⁴ (Fig. 4b, right). Here we analysed the cortical projection at P14, because MC targeting is completed at P14. However, OCAM staining was performed at P0, because OCAM expression decreases after birth. We also observed that the EYFP⁺ region is positive for *Nrp1*, a marker for MOB MCs (Supplementary Fig. 4d, left). Double ISH confirmed that *Nrp1* is expressed in the *Nrp2*⁺ MCs (Supplementary Fig. 4d, right). These results clearly demonstrate that *Nrp2*⁺ MCs in the MOB connect the PV-region MOB and anterior MeA.

Trans-synaptic labelling of MCs in the MOB. To examine whether anterior MeA neurons selectively receive afferent projections from the PV MOB, we performed monosynaptic labelling with the recombinant rabies virus (RV), which transmits across synapses in a retrograde direction⁴⁸. For the labelling of MCs, we used recombinant virus RV-ΔG-EGFP-EnvA that requires target cells to express avian receptor protein TVA and glycoprotein G for its selective infection, as well as monosynaptic transmission (Fig. 5a). We first injected adeno-associated virus (AAV) into the anterior side of MeA to complement TVA and glycoprotein G (Fig. 5b, left and Supplementary Fig. 5). After 2 weeks, RV-ΔG-EGFP-EnvA was injected into the same MeA region to selectively infect neurons expressing the TVA receptor. After 10 more days, serial sections of the entire MeA were analysed to confirm that the neurons infected with the AAV and RV were indeed confined to the MeA (Fig. 5b, left). We then examined the locations of EGFP-labelled MCs that were retrogradely infected with the RV. Eighty-one starter cells gave rise to 179 labelled MCs, 150 of which were specifically found in the PV MOB (Fig. 5b, right), suggesting that the MeA receives biased inputs from the PV MOB. For a control experiment, we injected the AAV and RV into the PIR, where 478 labelled MCs were generated from 98 starter cells in the PIR (Fig. 5c, left). No special preference was found in their locations in the MOB (Fig. 5c, right): EGFP-positive MCs are distributed randomly in the MOB as reported⁴⁹. These observations further support the idea that the anterior MeA receives MC projection from the MOB from the PV region.

Targeting of *Nrp2*⁺ MCs is also regulated by Sema3F. How do the *Nrp2*⁺ MCs project their axons from the PV MOB to the anterior MeA? To examine the possibility that *Nrp2* expressed by MCs plays a critical role in guiding axons, the MC-specific cKO of *Nrp2* was analysed at P14 for MC projection from the MOB. Since *Nrp2* signals are hardly detected at this stage, anti-*Nrp1*

Figure 3 | Sema3F co-regulates OSN projection and MC migration in the MOB. (a) Targeting of OSN axons and MC migration in the *Nrp2* KOs.

Parasagittal MOB sections at P0 were analysed by immunohistochemistry (upper panel). In the KOs, a coding sequence of the *Nrp2* has been deleted and replaced with that of *GFP*. Thus, OSNs that are supposed to express *Nrp2* can be detected with anti-*GFP* antibodies. Parasagittal sections at E18 were also analysed by *in situ* hybridization using the *GFP* and *Nrp2* probes (lower panel). Dotted lines in the enlarged photos indicate the boundary of the GL and MCL. $n = 7, 10, 6$ and 8 for the control, total KO, OSN-specific cKO and MC-specific cKO, respectively. (b) Targeting of OSN axons and MC migration in the *Sema3F* KOs. Parasagittal MOB sections at P0 were immunostained with anti-*Nrp2* antibodies (upper panel). In the *Sema3F* total KO and OSN-specific *Sema3F* conditional KO (OSN cKO), *Nrp2*⁺ OSNs are defasciculated and mistargeted to the dorsal MOB. Dotted lines in the enlarged photos indicate the boundary of the GL and MCL. Parasagittal MOB sections at E18 were also analysed by *in situ* hybridization with the *Nrp2* probe (lower panel). $n = 7, 9$ and 6 for the control, total KO and OSN-specific cKO, respectively. Scale bar, 200 μm. D, dorsal; V, ventral; A, anterior; P, posterior.

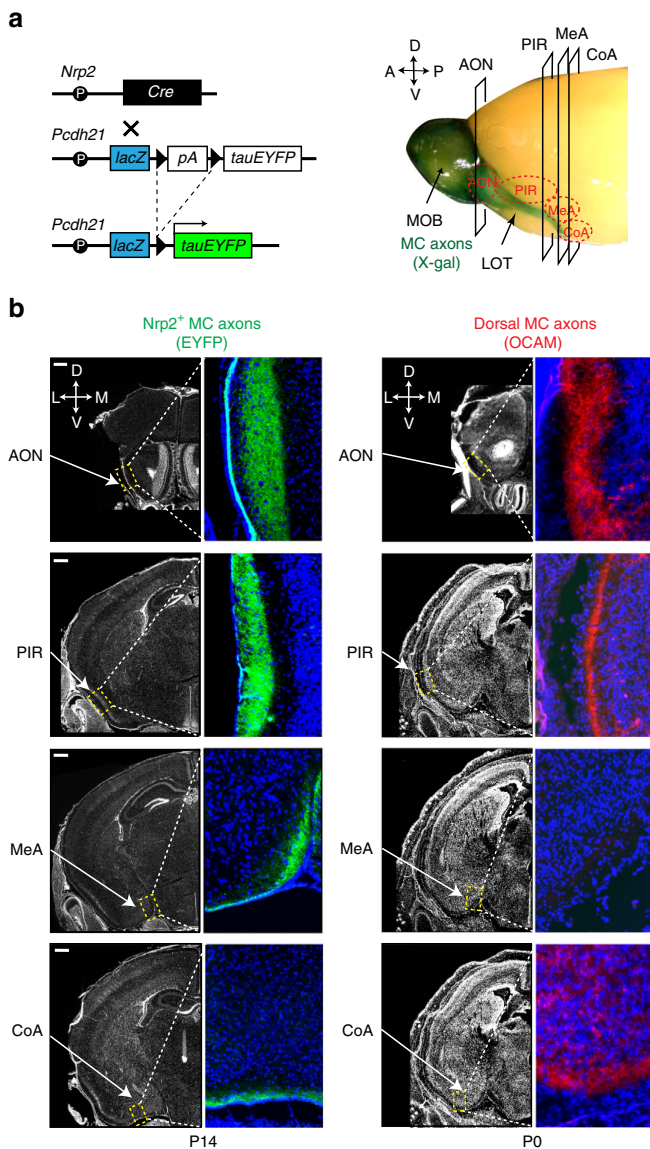


Figure 4 | Axonal projection of $Nrp2^+$ MCs to the MeA. (a) DNA constructs to detect the $Nrp2^+$ MC axons (left). The BAC Tg mouse $Nrp2$ -Cre was crossed with another Tg mouse $Pcdh21$ -lacZ-STOP-tauEYFP. Since $Nrp2$ was difficult to detect in MOB MCs, Tg mice, in which the $Nrp2$ -expressing MCs were labelled with EYFP, were generated. The $lacZ$ was inserted into the construct to detect the promoter activity of $Pcdh21$ by X-gal staining. Whole mount staining of the MOB is shown (right). Locations of coronal sections (AON, PIR and MeA) analysed in **b** are indicated. (b) Detection of $Nrp2^+$ MC axons in the OC. Coronal sections of the OC at P14 were immunostained with anti-GFP antibodies to detect EYFP expressed in the $Nrp2^+$ MCs (left). $Nrp2^+$ ventral MC axons (green) project to the AON, PIR, MeA and CoA. Coronal OC sections at P0 were immunostained with anti-OCAM antibodies (right). OCAM⁺ dorsal MC axons (red) project to the AON and PIR, but not to the MeA. $n=6$. Scale bar, 100 μ m. Nuclei are counterstained with DAPI in blue.

antibodies were used to detect MOB MC axons. Staining signals of $Nrp1$, a marker for MOB MCs, are severely reduced in the MeA of the $Nrp2$ KO, although signal levels are not changed in other OC regions (Fig. 6a and Supplementary Fig. 6). This observation demonstrates that the lack of $Nrp2$ leads to the dramatic decrease in the number of MC axons projecting from the MOB to the anterior MeA (Fig. 9a,c). A similar reduction is also found in the total KO of $Sema3F$, a repulsive ligand for $Nrp2$

(Fig. 6a,b). It is interesting that the axonal projection of $Nrp2^+$ MCs is not affected by the OSN-specific cKO of $Sema3F$ (Fig. 6a,b and Supplementary Fig. 7a), where the $Nrp2^+$ and $Nrp2^-$ MCs are not properly segregated within the MOB. This observation suggests that axonal projection of MCs to the anterior MeA takes place independent of their locations in the MOB (Fig. 9b). In the $Sema3F$ total KO, MCs in the AOB also fail to converge to the MeA and mistarget to the CoA (Supplementary Fig. 7b). Since $Sema3F$ is detected in the cortical regions surrounding the MeA (Fig. 7), $Nrp2^+$ MC axons are likely guided to the MeA by repulsive interactions with $Sema3F$ in the embryonic OC. Taken altogether, our results indicate that $Nrp2$ plays a dual instructive role in regulating MC migration within the MOB and in guiding axons of PV-region MCs to the anterior MeA through repulsive interactions with $Sema3F$ expressed in the dorsal MOB and outside regions of the MeA, respectively (Fig. 9a).

In utero electroporation of the human $Nrp2$ gene. Although we could demonstrate an essential role of $Nrp2$ in linking the PV MOB and anterior MeA, it was not clear whether the activation of $Nrp2$ is sufficient or any additional genes need to be activated in MCs to induce the circuit formation. To examine how much is regulated by $Nrp2$, we performed gain-of-function experiments by using *in utero* electroporation. A plasmid vector containing $EGFP$ cDNA was introduced into the WT embryonic OB with or without the human $Nrp2$ ($hNrp2$) cDNA. As reported previously⁵⁰, when the $EGFP$ was introduced alone at E11, immunostaining signals for $EGFP$ were equally distributed in both the dorsal and ventral regions of the MCL at P0 (Fig. 8a). In contrast, when the $hNrp2$ gene was co-transfected with $EGFP$, $EGFP^+$ cells were confined to the PV region in the MOB, as observed in MCs expressing endogenous $Nrp2$ (Fig. 8a). $EGFP^+$ cells were mostly positive for MC markers, $Tbr1$, $Tbr2$ and $Tbx21$ (Fig. 8a and Supplementary Fig. 8). This observation shows that constitutive expression of the exogenous $Nrp2$ gene is sufficient to bring MOB MCs to the PV region, even those that would normally remain in the dorsal MOB.

We then analysed axonal projections of MCs in the electroporated WT mice (Fig. 8b). $EGFP$ signals were not strongly found in the MeA when the $EGFP$ was electroporated without $hNrp2$ (Fig. 8b, upper left). In contrast, $EGFP$ signals were significantly increased in the anterior MeA at P0, when the $hNrp2$ was co-transfected with $EGFP$ (Fig. 8b, upper right). These experiments indicate that ectopic expression of $hNrp2$ can promote not only the migration of MCs to the PV MOB, but also their axonal projection to the anterior MeA. It is interesting that staining signals for OCAM, a dorsal MOB MC marker, were detected in the anterior MeA on the ipsilateral side of the MOB electroporated with $hNrp2$ cDNA (Fig. 8b, lower panel). This indicates that constitutive expression of exogenous $Nrp2$ alone can instruct axonal projection to the anterior MeA even in the dorsal lineage (OCAM⁺) MCs that do not normally send their axons to the anterior MeA. Taken together, these observations clearly demonstrate that activation of $Nrp2$ is not only necessary, but also sufficient to instruct circuit formation of MCs from the PV MOB to the anterior MeA.

Discussion

In the present study, we analysed roles of $Nrp2^+$ MCs in generating the neural circuit for attractive social responses. We previously reported that $Sema3F$ secreted by $Nrp2^-$ dorsal OSN axons directs late-arriving $Nrp2^+$ OSN axons to the PV MOB¹¹. The same dorsal OSN-derived $Sema3F$ was found to guide $Nrp2^+$ MCs from the ventricular zone to the PV region of MOB. This coordinated regulation of OSN projection and MC

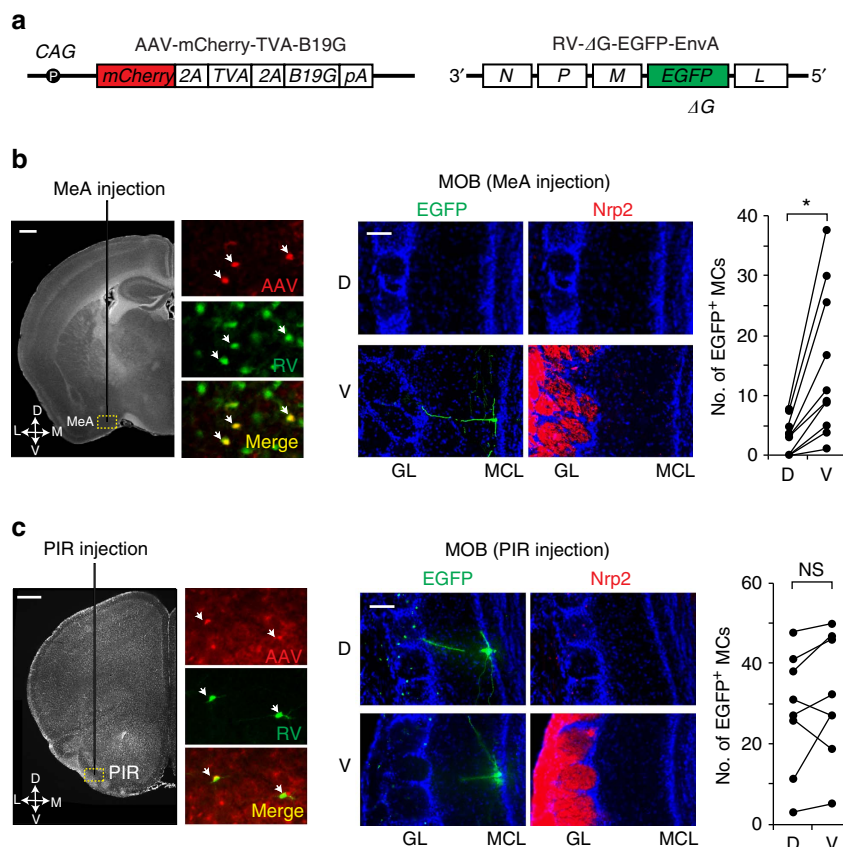


Figure 5 | Trans-synaptic tracing with the RV. (a) Virus constructs for circuit tracing. Structures of the AAV and RV are schematically shown. In the RV construct, the G region has been deleted (ΔG) and replaced with $EGFP^{51}$. (b) Virus injection into the MeA. AAV was first injected into the MeA region to complement TVA and glycoprotein G. After 2 weeks, the RV was injected into the same MeA region to selectively infect neurons expressing the TVA receptor. After 10 days, serial coronal sections of the entire MeA were analysed to determine whether the neurons infected with AAV and RV were indeed confined to the MeA. Double-labelled cells with mCherry for AAV and EGFP for RV are detected in the MeA. To detect the trans-synaptically labelled MCs, coronal sections of the MOB were immunostained with anti-GFP and anti-Nrp2 antibodies (right). EGFP-positive MCs are detected in the ventral (V), but not in the dorsal (D) region of the MOB. Numbers of EGFP-positive MCs in the dorsal (D) and ventral (V) MCs are compared in the right. Eighty-one starter MeA cells gave rise to 179 labelled MCs ($n = 10$ mice). $**P < 0.05$ (Wilcoxon signed-rank test). Scale bars, 200 μm (left) and 100 μm (right). (c) Virus injection to the PIR. Double-labelled cells with mCherry for AAV and EGFP for RV are detected in the PIR (left). To detect the trans-synaptically labelled MCs, coronal sections were immunostained with anti-GFP and anti-Nrp2 antibodies (right). EGFP-positive MCs are detected in both D and V regions of the MOB. Ninety-eight starter cells in the PIR resulted in 478 labelled MCs. $n = 8$ mice. NS: not significant (Wilcoxon signed-rank test). Scale bars, 200 μm (left) and 100 μm (right).

distribution appears to be key for functional pairing of OSN axons and MC dendrites in the MOB. We further examined targeting of $Nrp2^+$ MCs localized to the PV MOB. In a previous report⁵¹, dye-injection experiments indicated that the MeA receives MC inputs not only from the AOB, but also from the MOB. By using fluorescent tags, we found that $Nrp2^+$ MCs send their axons to the anterior portion of MeA. Furthermore, retrograde virus tracing revealed that $Nrp2^+$ MCs in the PV MOB do indeed form synapses with MeA neurons.

Our gain-of-function (*in utero* electroporation) and loss-of-function (KO) experiments demonstrate that $Nrp2$ - $Sema3F$ repulsive interactions are essential not only for guiding $Nrp2^+$ MCs to the PV MOB, but also for instructing their axons to the anterior MeA (Fig. 9). In the *in utero* electroporation experiment, MCs expressing hNrp2 with EGFP are not only guided to the PV MOB, but also instructed to send their axons to the anterior MeA. In the electroporated mice, the EGFP⁺ (hNrp2⁺) region in the anterior MeA became positive for the dorsal MC marker, OCAM. These results demonstrate that ectopic expression of hNrp2 in the mouse MCs is sufficient to instruct their circuit formation to the anterior MeA even in dorsal lineage MCs. It will be interesting to

study whether these transfected neurons form functional circuits receiving OSN input from the OB and making synaptic connections to the anterior MeA.

In the $Nrp2$ total KO and MC-specific cKO, signals of MC axons projecting from the MOB are significantly reduced in the anterior MeA, and a similar phenotype is observed in the $Sema3F$ total KO. MCs that were supposed to project to the MeA may reroute their axons targeting to other areas in the OC or simply do not survive during development. Since $Sema3F$ is expressed in the cortical regions surrounding the MeA during early embryonic development, $Nrp2^+$ MC axons are likely driven to the MeA by repulsive interactions with $Sema3F$ expressed just outside their trajectory. It seemed puzzling that $Nrp2^+$ MCs targeted their collaterals to the $Sema3F^+$ areas in the OC at later stages of development. However, this can be explained by the temporal regulation of $Nrp2$ and $Sema3F$ expression: Both $Nrp2$ and $Sema3F$ are expressed at embryonic stages (E12–18), but disappear later on when collateral extension starts to occur. It has been reported that the D–V topography in the OB is roughly correlated with that in the AON pars externa but not in the PIR^{49,52–54}. Furthermore, incoming odour signals in the CoA are

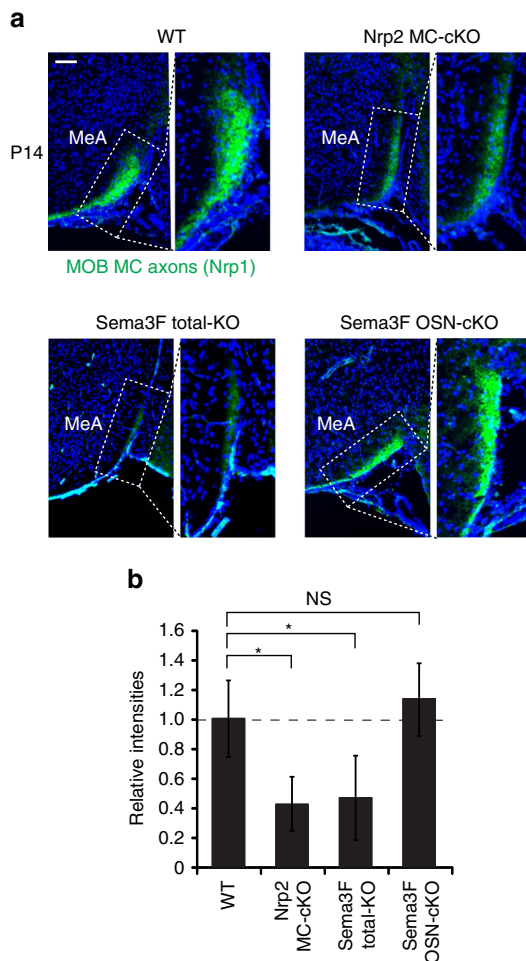


Figure 6 | MC projection to the MeA is regulated by the Nrp2/Sema3F signalling. (a) Detection of Nrp2⁺ MC axons in the MeA. MC axons projecting from the MOB at P14 are stained green with anti-Nrp1 antibodies. Since Nrp2 signals in MOB MCs are hardly detected at this stage, anti-Nrp1 antibodies were used to detect MOB MC axons. Targeting of Nrp1⁺ MC axons to the MeA is affected in the MC-specific cKO of Nrp2 and Sema3F total KO, but not in the OSN-specific Sema3F cKO (OSN cKO). Scale bar, 200 μ m. (b) Nrp1 signals in the MeA. Intensities of green staining (Nrp1⁺) in the anterior MeA are compared between the WT and various KOs. Nrp1 signals are reduced nearly by half in the MC-specific cKO of Nrp2 or Sema3F, but not in the OSN-specific cKO of Sema3F. * $P < 0.01$, NS: not significant (Student's *t*-test). $n = 5$ for each genotype.

mostly from the dorsal OB^{49,53}. Keeping these previous observations in mind, we closely analysed the secondary projection of Nrp2⁺ MCs to the AON, PIR, MeA and CoA. We found that Nrp2⁺ MCs in the PV OB preferentially target their axons to the anterior MeA, although they send their axons to the AON, PIR and CoA as well.

MCs exhibit a protracted waiting period before sending their collateral branches to the target. It has been reported that the target OC in culture becomes accessible to MC fibres at E16.5 during development⁵⁵. Innervation in the central areas is completed by PD15. First collaterals are extended towards the AON and PIR at E16.5, and innervation to the OT is completed after birth^{55,56}. Despite these previous studies, timing of innervation to the MeA was still unclear. Our study demonstrates that Nrp2 instructs targeting of ventral MCs to the MeA. During development, Nrp2 is expressed in the ventral MCs at embryonic stages, but disappears by PD14. It is likely that innervation to the MeA occurs at embryonic stages.

The MeA is known to process non-volatile pheromone signals, detected by the VNO, to induce innate social behaviours, such as mating, conspecific recognition and fear responses^{16,20,21,57,58}. Previous dye-injection experiments suggested that the MeA also receive MOB inputs in the anterior regions⁵¹. Furthermore, a surgical lesion to the anterior MeA of the hamster has been shown to abolish the males' preference for female urine over that of males¹⁶. Our present study demonstrates that it is the Nrp2⁺ subset of MCs that sends attractive social inputs from the PV MOB to the anterior MeA. In the MC-specific cKO of Nrp2, AOB-independent social behaviours are affected. For example, pup suckling and male vocalization are impaired in the cKO. It is generally accepted that the AOB detects non-volatile social cues to induce various innate behaviours, whereas the MOB detects volatile odour ligands⁵⁹. During evolution, the mammalian olfactory system rapidly expanded the MOB structure to accommodate greater numbers of glomeruli for class II ORs devoted to volatile odorants in the ventral region⁶⁰. It is probable that the MOB developed a subset of Nrp2⁺ MCs that allowed axons to project to the MeA using the Nrp2/Sema3F guidance system, similar to the AOB. This may have conferred the evolutionary advantage of detecting volatile social cues from distances. It is quite possible that the main olfactory system governs attractive social responses, even in the human whose VNO no longer has any function and vomeronasal-receptor genes have all become pseudogenes^{61,62}.

It is rather surprising that activation of a single axon guidance gene, *Nrp2*, in immature MCs is sufficient to instruct their neural circuit formation to the anterior MeA. Our present study clearly demonstrates that Nrp2⁺ MCs in the PV MOB play a critical role in inducing attractive social responses. These findings demonstrate a close correlation between functional domains in the MOB and specific regions in the OC (Fig. 9d). We assume that this is accomplished by gathering glomeruli with the same behavioural quality to a restricted area (functional domain) in the MOB. It is also important for MCs to ensure that the olfactory inputs with the same odour quality, regardless of their chemical nature, are transmitted to a specific region in the OC so that they could induce the same type of outputs. For attractive social responses, Nrp2 is a key determinant for connecting the PV MOB and anterior MeA by using a specific subset of MCs.

It is quite possible that this kind of circuit formation observed in MCs, which is directed by a distinct set of guidance molecules, is a general rule that is applicable to other innate odour responses. For example, fear to predators' smell and avoidance to spoiled food odours are induced by activation of glomeruli located in the avoidance (D_I) and fear (D_{II}) domains in the MOB, respectively¹⁴. Furthermore, the CoA is reported to play an important role in inducing aversive responses to fox odour TMT¹⁵. It will be interesting to determine which axon guidance system is responsible for establishing the MC circuits connecting the dorsal MOB and CoA. In summary, it has become clear in the present study that activation of a single guidance gene, *Nrp2*, could determine a functional lineage of MCs and is sufficient to instruct circuit formation between the MOB and OC for attractive social behaviours.

Methods

Mice. Tg Goofy-Cre⁶³ and Tg AP2 ϵ -Cre³⁰ mice were obtained from Y. Yoshihara and T. Williams, respectively. The Nrp2-floxed, Sema3F-floxed, Rosa26-STOP-lacZ and Eno2-Cre mice were purchased from The Jackson Laboratory. Goofy-Cre, AP2 ϵ -Cre and Eno2-Cre mice were crossed with the Nrp2- or Sema3F-floxed mice to generate the OSN-specific, MC-specific and total KO mice, respectively. To generate the Nrp2-Cre construct, the BAC clone RP24-250G22 containing the Nrp2 promoter was modified and the *NiCre-pA-rpsL* sequence was introduced into the translation start site of Nrp2, using the Counter-Selection BAC Modification Kit (GENE BRIDGES). In the *Pcdh21* gene, an enhancer/promoter site was identified at ~10 kb upstream of the coding region⁶⁴. The 10 kb fragment of *Pcdh21* was isolated from the BAC clone and introduced into the SKA vector. The *intron-tau-lacZ-STOP-ires-tauEYFP-pA* sequence was inserted into the *Pcdh21* minigene. Mice

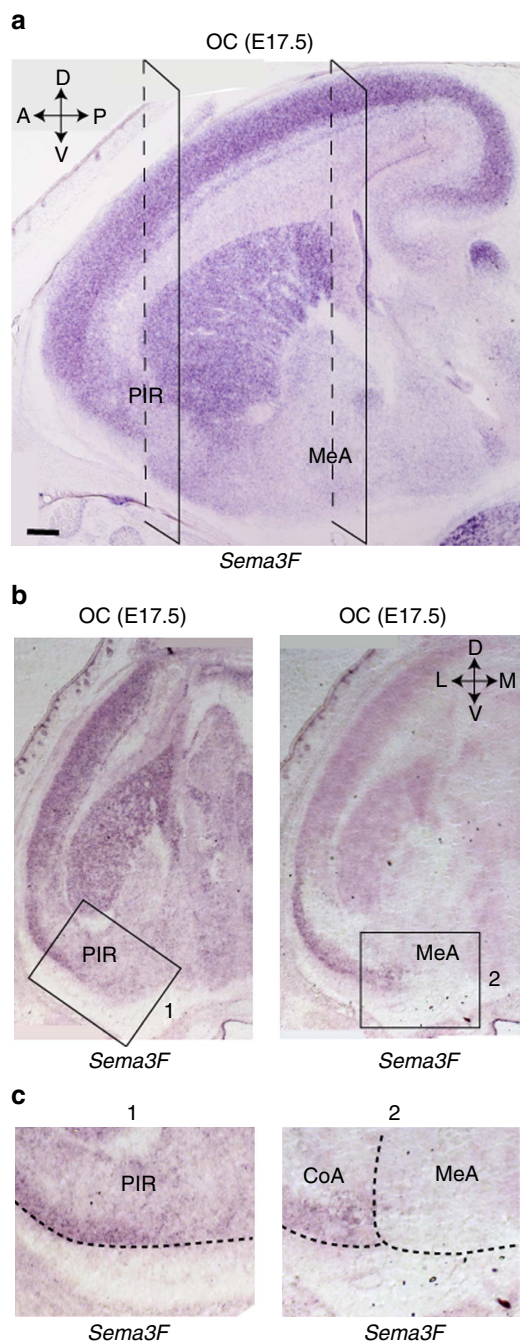


Figure 7 | *In situ* hybridization of *Sema3F* expression in the OC.

(a) A parasagittal section at E17.5 was hybridized with the *Sema3F* probes. (b) Coronal OC sections containing the PIR and MeA in a were analysed. *Sema3F* transcripts are high in the PIR, but rarely detected in the MeA at the early embryonic stage. (c) Enlarged photos of PIR (1) and MeA (2) are shown in b. Scale bar, 200 μm.

were housed in a 12-h light/dark schedule and had free access to the food and water. Sample sizes were determined based on the standard procedure. No method was used to randomize the animals among the experimental group. The investigator was not blinded to the genotype, except for the pup suckling. Animal experiments were performed in accordance with the guideline of Animal Care Committees in the University of Tokyo, University of Fukui, Azabu University and RIKEN Institute in Kobe.

Two-choice preference test. We used an acrylic box (300 × 150 × 155 mm) containing three compartments—one is for mice (95 × 130 mm) and two are for samples (190 × 65 mm). Urine samples were collected for 5 consecutive days from

10 male and 10 female mice. Each sample (60 μl) was spotted on a filter paper (40 × 40 mm) and placed in a sample compartment. The partition had a vent to allow air to pass and mice to poke their snouts through. An air stream was drawn through a charcoal filter from each sample compartment to the mouse compartment with a vacuum pump. In the preference test, MC-specific Nrp2 cKO and littermate male (8–12 weeks old) were analysed. Each adult mouse was habituated for 5 min before the test. During subsequent 5 min, the time amount that a mouse spent in poking its nose was measured (investigation time). The mouse behaviour was recorded with a digital video camera.

MTMT preference test. Castrated male urine was collected from five animals. Sexually experienced female mice were used to analyse the behavioural effects of MTMT in a urine preference test¹⁷. A piece of filter paper spotted with 50 μl of castrated male urine alone or castrated male urine with 20 ppb MTMT was presented to the MC-specific Nrp2 cKO and littermate mice (8–12 weeks old). Each adult mouse was habituated for 5 min before the test. In the subsequent 5-min duration, the amount of time spent for poking the nose was measured (investigation time). The animal behaviour was recorded with a digital video camera.

Recording of ultrasonic vocalization. USV was detected using a condenser microphone (UltraSoundGate CM16/CMPA, Avisoft Bioacoustics) that was connected to an A/D converter (UltraSoundGate 116; Avisoft Bioacoustics) with a sampling rate of 400 kHz. Acoustic signals were transmitted to a vocalization analysis system (SASLab Pro; Avisoft Bioacoustics). Both Nrp2 MC-specific Nrp2 cKO and littermate male (8–12 weeks old) were analysed. $n = 10$ for each genotype. Each adult male was habituated for 5 min before the test. The vocalization was recorded for 6 min and the number of USVs was counted.

Viral injection. The mutant RV-ΔG-EGFP was obtained from Dr Callaway, and amplified. RV-ΔG-EGFP-EnvA was produced as follows. BHK-EnvARGCD cells were plated in 12-well plates at 2E5 cells per well. The following day, the glycoprotein-deleted RV SADDG-EGFP was added at a multiplicity of infection (MOI) of 1.5. The following day, the cells in each well were trypsinized and replated into a 10 cm plate. Virus-containing supernatants were collected 2 days later, filter sterilized and frozen at 80 °C in 1 ml aliquots⁴⁸. The AAV vector encoding TVA, rabies glycoprotein and mCherry (pFBAAV-CAG-mCherry-TVA-B19G), was constructed from pAAV-EF1a-FLEX-GTB (a kind gift from Dr Callaway), followed by viral packaging in Sf9 cells and purification as described⁴⁵. For trans-synaptic labelling, 0.5 μl of AAV2/1-CAG-mCherry-TVA-B19G (2.0×10^{12} genome copy ml⁻¹) was injected into the brain at P60. During surgery, animals were anaesthetized with 400 mg kg⁻¹ chloral hydrate and 44 mg kg⁻¹ xylazine. For injection to the MeA, a needle was placed A/P - 1.04 mm, M/L - 1.9 mm from the bregma, D/V - 5.4 mm from the surface. For injection to the PIR, a needle was placed A/P + 1.5 mm, M/L - 2.5 mm from the bregma, D/V - 4.8 mm from the surface. After 2 weeks, RV-ΔG-EGFP-EnvA (10^7 – 10^8 plaque forming unit ml⁻¹) was injected into the same coordinate, MeA or PIR. Animals were then housed for 10 days to allow the virus to infect and spread trans-synaptically.

In utero electroporation. For *in utero* electroporation, pregnant mice were anaesthetized by intraperitoneal injection of ketamine (100 mg kg⁻¹) and xylazine (10 mg kg⁻¹). The uterine horns were removed from the abdominal cavity⁵⁰. Approximately 0.5 μl of DNA solution (1.5–4 μg μl⁻¹ in 50% TE) was injected into the lateral cerebral ventricle of embryos. DNA solution was mixed with Fast Green (100 μg ml⁻¹) to visualize the injection site. Electroporation was performed by applying square electric pulses. Two pulses of 30 V were given for 50 ms with a 950 ms interval. Positive current was given from posterior to anterior in the MOB to efficiently label the MC precursors. The uterine horns were repositioned in the abdominal cavity.

Suckling behaviour of pups. Lactating female mice were anaesthetized and laid on the side exposing nipples towards pups. P0 pups were fasted for 4 h before the experiment, and placed 1 cm away from the female's nipple. The time for finding nipples to suckle was measured within 4 min. Each pup was used only once in one stimulus condition. Experiments were performed in blind to the genotype of pups. The genotype was examined after each experiment.

Fear responses to TMT. Mice were habituated to a clean cage (23 × 16 × 12 cm) for 5 min before the test. A piece of filter paper spotted with 10 μl of undiluted TMT (Contech Enterprise Inc.) was presented to mice for 10 min. MC-specific Nrp2 cKO and littermate mice (8–12 weeks old) were analysed. $n = 10$ for each genotype. The mouse behaviour was recorded with a digital video camera. Average freezing time was measured.

Habituation-dishabituation test. A small perforated tube (1.5 ml microtube) with a piece of cotton spotted with 10 μl of 1% vanillin (or undiluted α-terpinene) was presented to the mouse for 1 min. This was repeated four times with 10-min

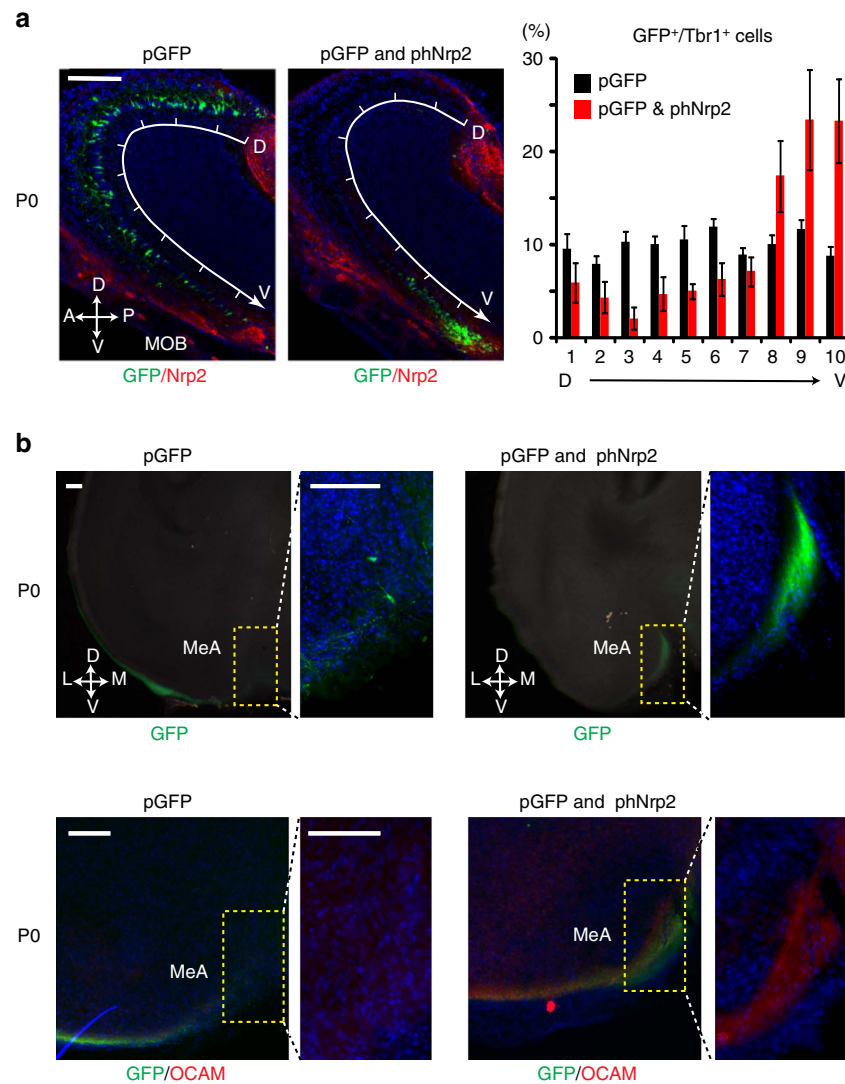


Figure 8 | *In utero* electroporation of the *Nrp2* gene. (a) *In utero* electroporation of the embryonic MOB. Plasmid vectors containing *EGFP* cDNA (pGFP) with or without human *Nrp2* cDNA (phNrp2) were introduced into the MOB at E11. Parasagittal MOB sections at P0 were immunostained with antibodies against GFP (to detect ectopic hNrp2⁺ MCs) and mouse *Nrp2* (to detect endogenous Nrp2⁺ MCs) (left). Note that the anti-mouse *Nrp2* antibodies do not detect the human *Nrp2*. The MOB was dissected into 10 sections along the D–V axis and the distribution of GFP⁺ Tbr1⁺ MCs was analysed. Statistical data are shown in the right. Ectopic expression of *Nrp2* alone appears to direct migration of EGFP⁺ MCs to the PV MOB. Data are presented in mean \pm s.e. Scale bar, 200 μ m. (b) Projection of electroporated hNrp2⁺ MCs to the MeA. Coronal sections of the OC at P0 were immunostained with anti-GFP (green) and anti-OCAM antibodies (red). Note that the dorsal MC marker (OCAM) is detected with EGFP in the MeA, when the hNrp2 is ectopically expressed in MCs. Scale bar, 100 μ m. Nuclei are counterstained with DAPI in blue (a,b).

intervals. In the fifth trial 10 min later, a 10 μ l drop of undiluted α -terpinene (or 50 mM, 0.5 μ M vanillin) was placed in the mouse cage. Habituation is defined by the progressive decrease of sniffing towards the repeated presentation of the same odour. Dishabituation is refined by the reinstatement of sniffing when the novel odour is presented. MC-specific cKO of *Nrp2* and littermate mice (8–12 weeks old) were analysed. $n = 6$ and 4 for each genotype in the 50 mM and 0.5 μ M vanillin experiments, respectively.

***In situ* hybridization.** After perfusion with 4% paraformaldehyde (PFA) in phosphate-buffered saline (PBS), the brain samples were taken out from mice and fixed overnight with 4% PFA in PBS. Parasagittal or coronal sections (10–20 μ m each) were prepared from the frozen tissues in OCT compound (Tissue-Tek). To generate RNA probes, DNA fragments of 500–1,000 bp were amplified from cDNA of the mouse brain (C57BL/6). PCR products were subcloned into pGEM-T (Promega) and used as templates for RNA probes. To label the probes with digoxigenin (DIG), the DIG RNA labelling kit (Roche) was used. For *in situ* hybridization, samples were fixed in 4% PFA for 15 min at 4 $^{\circ}$ C (refs 11,66). After rinsing with PBS, the sections were incubated with 7 μ g ml⁻¹ proteinase K for 10 min at 37 $^{\circ}$ C. The samples were fixed again with 4% PFA in PBS for 10 min, incubated with 0.25% acetic anhydride and 0.1 M triethanolamine, pH 8.0 and

washed with PBS. For hybridization, the sections were incubated for 16 h at 51 $^{\circ}$ C with probes. After washing, the samples were blocked with the blocking reagent (Roche), and incubated with the alkaline phosphatase (AP)-conjugated anti-DIG antibody (Roche). Probe-positive cells were stained purple with nitroblue tetrazolium salt and 5-bromo-4-chloro-3-indolyl phosphate toluidinium salt. For fluorescence staining, probe-positive cells were incubated with a HNPP/FastRed (Roche) in the staining buffer (100 mM Tris-Cl pH 8.0, 100 mM NaCl, 5 mM MgCl₂). After washing, samples were photographed with a confocal microscope, model BX61 (Olympus). Boundaries of brain structures were determined according to the standard atlas^{67,68}.

Immunohistochemistry. Immunohistochemistry was performed according to the published procedure¹² using the following antibodies: anti-Nrp1 (1:500; R&D systems), anti-Nrp2 (1:500; R&D systems), anti-GFP (1:1,000; Clontech), anti- β -galactosidase (1:1,000; ICN Biochemicals), anti-OCAM (1:500; R&D systems), rabbit anti-Tbr1 (1:5,000; Abcam), rabbit anti-Tbr2 (1:5,000; Abcam), anti-BrdU (1:200; Abcam) and rabbit anti-Tbx21 (1:10,000; provided by Dr Yoshihara at RIKEN). Antibodies against *Pcdh21* were generated by immunizing guinea pigs with KLH-conjugated synthetic peptides as described previously¹¹. Alexa fluor-conjugated secondary antibodies (Invitrogen) were used at 1:200 dilution.

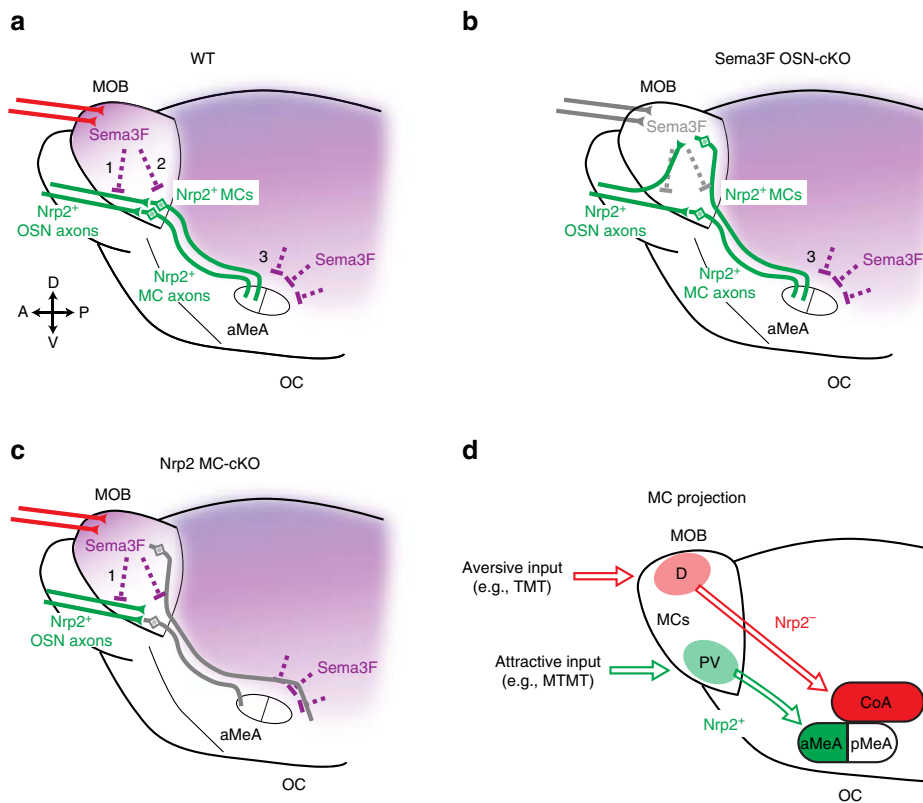


Figure 9 | Schematic diagrams of *Nrp2*⁺ MC targeting. (a) Sema3F–*Nrp2* interactions in the olfactory circuit formation in the WT. A repulsive ligand, Sema3F, expressed by the dorsal-region OSNs is essential for guiding both *Nrp2*⁺ OSN axons (1) and *Nrp2*⁺ MCs to the ventral OB (2). OC-region Sema3F instructs axon targeting of *Nrp2*⁺ MCs to the MeA (3). (b) Targeting of *Nrp2*⁺ MCs in the OSN-specific Sema3F cKO. Because of the absence of Sema3F in the dorsal MOB (1), distribution of *Nrp2*⁺ MCs (2) is perturbed. However, targeting of *Nrp2*⁺ MCs (3) to the anterior MeA (aMeA) is not affected. *Nrp2*⁺ MCs remaining in the dorsal MOB in the cKO send their axons to the aMeA. (c) Targeting of MCs in the MC-specific *Nrp2* cKO. Because of the absence of *Nrp2* in MCs, both distribution (2) and targeting (3) of MCs are impaired in the cKO. MC axons from the MOB are significantly reduced in the aMeA. (d) A schematic diagram of the secondary projection in the mouse olfactory system. Aversive signals are reported to be transmitted from the dorsal MOB to the CoA^{14,15}. *Nrp2*⁺ MCs convey the attractive social signals from the PV MOB to the aMeA but not to the posterior region (pMeA). Our present study revealed that activation of a single axon guidance gene, *Nrp2*, in MCs is sufficient to instruct olfactory circuit formation from the MOB to MeA.

X-gal staining. Olfactory tissues were prepared after perfusion with 4% PFA in PBS. The sections were washed with PBS and placed in X-gal staining buffer (5 mM potassium ferricyanide, 5 mM potassium ferrocyanide, 2 mM MgCl₂, 0.01% sodium deoxycholate, 0.02% Nonidet P-40 (NP-40), 1 mg ml⁻¹ X-gal in PBS). The samples were incubated overnight at 37 °C in the dark. Photographs were taken with an Olympus Optical AX70 microscope (Olympus).

BrdU labelling. Labelling of 5-bromodeoxyuridine (BrdU) was performed as described previously⁶⁹. BrdU was intraperitoneally injected into the pregnant mice (100 mg kg⁻¹) at pregnant day 9, 10, 11, 12, 13 and 14. OB sections were prepared from the E18.5 embryo, and washed three times with PBS at room temperature for 5 min, incubated in 1.2 N HCl at 37 °C for 1 h, rinsed in 100 mM borate buffer (pH 8.5) at room temperature for 1 min twice and in PBS briefly. Then, the BrdU was stained with anti-BrdU antibodies.

Plasmids. A plasmid vector containing the *egfp* cDNA with CAG enhancer (pGFP) was obtained from Addgene (pCAG-GFP; Plasmid #11150). To construct p*Nrp2*, full-length human *nrp2* cDNA was cloned with PCR using the template plasmid (Clone; HsCD00443185) from DNASU. Primer sequences used were: 5'-AGTGATATCCACCATGGATATGTTTCCTCTCACC-3'; and 5'-AGTGATATCTCATGCCTCGGAGCAGCACTTTTGG-3'. The obtained PCR fragment was inserted into the pCAGEN vector (Addgene; Plasmid #11160).

Intensity measurements and statistical analyses. Optical images were photographed with an Olympus Optical AX70 microscope. Sections were also analysed by a fluorescence microscope, Olympus model IX70 equipped with a cooled CCD camera, C4742-95-12ERG (Hamamatsu Photonics). For quantification of signals, the tone was reversed and monochrome images were used. Staining intensities were

measured with ImageJ. Statistical analyses were performed with Excel 2010 (Microsoft).

Data availability. The data that support the findings in this study are available from the corresponding author on request.

References

- Doty, R. L. Odor-guided behavior in mammals. *Experientia* **42**, 257–271 (1986).
- Buck, L. & Axel, R. A novel multigene family may encode odorant receptors: a molecular basis for odor recognition. *Cell* **65**, 175–187 (1991).
- Vassar, R. *et al.* Topographic organization of sensory projections to the olfactory bulb. *Cell* **79**, 981–991 (1994).
- Ressler, K. J., Sullivan, S. L. & Buck, L. B. Information coding in the olfactory system: evidence for a stereotyped and highly organized epitope map in the olfactory bulb. *Cell* **79**, 1245–1255 (1994).
- Mombaerts, P. *et al.* Visualizing an olfactory sensory map. *Cell* **87**, 675–686 (1996).
- Shipley, M. T. & Adamek, G. D. The connections of the mouse olfactory bulb: a study using orthograde and retrograde transport of wheat germ agglutinin conjugated to horseradish peroxidase. *Brain Res. Bull.* **12**, 669–688 (1984).
- Schwob, J. E. & Price, J. L. The development of axonal connections in the central olfactory system of rats. *J. Comp. Neurol.* **223**, 177–202 (1984).
- Giger, R. J. *et al.* Neuropilin-2 is a receptor for semaphorin IV: insight into the structural basis of receptor function and specificity. *Neuron* **21**, 1079–1092 (1998).
- Imai, T. *et al.* Pre-target axon sorting establishes the neural map topography. *Science* **325**, 585–590 (2009).

10. Kolodkin, A. L. *et al.* Neuropilin is a semaphorin III receptor. *Cell* **90**, 753–762 (1997).
11. Takeuchi, H. *et al.* Sequential arrival and graded secretion of Sema3F by olfactory neuron axons specify map topography at the bulb. *Cell* **141**, 1056–1067 (2010).
12. Serizawa, S. *et al.* A neuronal identity code for the odorant receptor-specific and activity-dependent axon sorting. *Cell* **127**, 1057–1069 (2006).
13. Mori, K. & Sakano, H. How is the olfactory map formed and interpreted in the mammalian brain? *Annu. Rev. Neurosci.* **34**, 467–499 (2011).
14. Kobayakawa, K. *et al.* Innate versus learned odour processing in the mouse olfactory bulb. *Nature* **450**, 503–508 (2007).
15. Root, C. M., Denny, C. A., Hen, R. & Axel, R. The participation of cortical amygdala in innate, odour-driven behaviour. *Nature* **515**, 269–273 (2014).
16. Maras, P. M. & Petrucci, A. Chemosensory and steroid-responsive regions of the medial amygdala regulate distinct aspects of opposite-sex odor preference in male Syrian hamsters. *Eur. J. Neurosci.* **24**, 3541–3552 (2006).
17. Lin, D. Y., Zhang, S. Z., Block, E. & Katz, L. C. Encoding social signals in the mouse main olfactory bulb. *Nature* **434**, 470–477 (2005).
18. Yoshikawa, K., Nakagawa, H., Mori, N., Watanabe, H. & Touhara, K. An unsaturated aliphatic alcohol as a natural ligand for a mouse odorant receptor. *Nat. Chem. Biol.* **9**, 160–162 (2013).
19. Duan, X. *et al.* Crucial role of copper in detection of metal-coordinating odorants. *Proc. Natl Acad. Sci. USA* **109**, 3492–3497 (2012).
20. Lehman, M. N., Winans, S. S. & Powers, J. B. Medial nucleus of the amygdala mediates chemosensory control of male hamster sexual behavior. *Science* **210**, 557–560 (1980).
21. DiBenedictis, B. T., Ingraham, K. L., Baum, M. J. & Cherry, J. A. Disruption of urinary odor preference and lordosis behavior in female mice given lesions of the medial amygdala. *Physiol. Behav.* **105**, 554–559 (2012).
22. Keller, M., Douhard, Q., Baum, M. J. & Bakker, J. Destruction of the main olfactory epithelium reduces female sexual behavior and olfactory investigation in female mice. *Chem. Senses* **31**, 315–323 (2006).
23. Martel, K. L. & Baum, M. J. Sexually dimorphic activation of the accessory, but not the main, olfactory bulb in mice by urinary volatiles. *Eur. J. Neurosci.* **26**, 463–475 (2007).
24. Kimchi, T., Xu, J. & Dulac, C. A functional circuit underlying male sexual behaviour in the female mouse brain. *Nature* **448**, 1009–1014 (2007).
25. Leybold, B. G. *et al.* Altered sexual and social behaviors in trp2 mutant mice. *Proc. Natl Acad. Sci. USA* **99**, 6376–6381 (2002).
26. Stowers, L., Holy, T. E., Meister, M., Dulac, C. & Koentges, G. Loss of sex discrimination and male-male aggression in mice deficient for TRP2. *Science* **295**, 1493–1500 (2002).
27. Mandiyan, V. S., Coats, J. K. & Shah, N. M. Deficits in sexual and aggressive behaviors in Cnga2 mutant mice. *Nat. Neurosci.* **8**, 1660–1662 (2005).
28. Inaki, K., Nishimura, S., Nakashiba, T., Itoharu, S. & Yoshihara, Y. Laminar organization of the developing lateral olfactory tract revealed by differential expression of cell recognition molecules. *J. Comp. Neurol.* **479**, 243–256 (2004).
29. Walz, A., Rodriguez, I. & Mombaerts, P. Aberrant sensory innervation of the olfactory bulb in neuropilin-2 mutant mice. *J. Neurosci.* **22**, 4025–4035 (2002).
30. Feng, W., Simoes-de-Souza, F., Finger, T. E., Restrepo, D. & Williams, T. Disorganized olfactory bulb lamination in mice deficient for transcription factor AP-2 ϵ . *Mol. Cell. Neurosci.* **42**, 161–171 (2009).
31. Feng, W. & Williams, T. Cloning and characterization of the mouse AP-2 ϵ gene: a novel family member expressed in the developing olfactory bulb. *Mol. Cell. Neurosci.* **24**, 460–475 (2003).
32. Tummalala, R., Romano, R. A., Fuchs, E. & Sinha, S. Molecular cloning and characterization of AP-2 ϵ , a fifth member of the AP-2 family. *Gene* **321**, 93–102 (2003).
33. Schaefer, M. L., Young, D. A. & Restrepo, D. Olfactory fingerprints for major histocompatibility complex-determined body odors. *J. Neurosci.* **21**, 2481–2487 (2001).
34. Nyby, J., Wysocki, C. J., Whitney, G. & Dizinno, G. Pheromonal regulation of male mouse ultrasonic courtship (*Mus musculus*). *Anim. Behav.* **25**, 333–341 (1977).
35. Hudson, R. & Distel, H. Pheromonal release of suckling in rabbits does not depend on the vomeronasal organ. *Physiol. Behav.* **37**, 123–128 (1986).
36. Garrosa, M., Gayoso, M. J. & Esteban, F. J. Prenatal development of the mammalian vomeronasal organ. *Microsc. Res. Tech.* **41**, 456–470 (1998).
37. Oka, Y. *et al.* Odorant receptor map in the mouse olfactory bulb: *in vivo* sensitivity and specificity of receptor-defined glomeruli. *Neuron* **52**, 857–869 (2006).
38. McBride, K. & Slotnick, B. Discrimination between the enantiomers of carvone and of terpinen-4-ol odorants in normal rats and those with lesions of the olfactory bulbs. *J. Neurosci.* **26**, 9892–9901 (2006).
39. Hinds, J. W. Autoradiographic study of histogenesis in the mouse olfactory bulb. I. Time of origin of neurons and neuroglia. *J. Comp. Neurol.* **134**, 287–304 (1968).
40. Blanchart, A., De Carlos, J. A. & Lopez-Mascaraque, L. Time frame of mitral cell development in the mice olfactory bulb. *J. Comp. Neurol.* **496**, 529–543 (2006).
41. Suarez, R., Garcia-Gonzalez, D. & de Castro, F. Mutual influences between the main olfactory and vomeronasal systems in development and evolution. *Front. Neuroanat.* **6**, 50 (2012).
42. Devor, M. Fiber trajectories of olfactory bulb efferents in the hamster. *J. Comp. Neurol.* **166**, 31–47 (1976).
43. Yoshihara, Y. *et al.* A genetic approach to visualization of multisynaptic neural pathways using plant lectin transgene. *Neuron* **22**, 33–41 (1999).
44. Treloar, H. B., Gabeau, D., Yoshihara, Y., Mori, K. & Greer, C. A. Inverse expression of olfactory cell adhesion molecule in a subset of olfactory axons and a subset of mitral/tufted cells in the developing rat main olfactory bulb. *J. Comp. Neurol.* **458**, 389–403 (2003).
45. Dulac, C. & Torello, A. T. Molecular detection of pheromone signals in mammals: from genes to behaviour. *Nat. Rev. Neurosci.* **4**, 551–562 (2003).
46. Scalia, F. & Winans, S. S. The differential projections of the olfactory bulb and accessory olfactory bulb in mammals. *J. Comp. Neurol.* **161**, 31–55 (1975).
47. de Olmos, J., Hardy, H. & Heimer, L. The afferent connections of the main and the accessory olfactory bulb formations in the rat: an experimental HRP-study. *J. Comp. Neurol.* **181**, 213–244 (1978).
48. Wickersham, I. R. *et al.* Monosynaptic restriction of transsynaptic tracing from single, genetically targeted neurons. *Neuron* **53**, 639–647 (2007).
49. Miyamichi, K. *et al.* Cortical representations of olfactory input by trans-synaptic tracing. *Nature* **472**, 191–196 (2011).
50. Imamura, F. & Greer, C. A. Segregated labeling of olfactory bulb projection neurons based on their birthdates. *Eur. J. Neurosci.* **41**, 147–156 (2015).
51. Kang, N., Baum, M. J. & Cherry, J. A. A direct main olfactory bulb projection to the 'vomeronasal' amygdala in female mice selectively responds to volatile pheromones from males. *Eur. J. Neurosci.* **29**, 624–634 (2009).
52. Yan, Z. *et al.* Precise circuitry links bilaterally symmetric olfactory maps. *Neuron* **58**, 613–624 (2008).
53. Sosulski, D. L., Bloom, M. L., Cutforth, T., Axel, R. & Datta, S. R. Distinct representations of olfactory information in different cortical centres. *Nature* **472**, 213–216 (2011).
54. Ghosh, S. *et al.* Sensory maps in the olfactory cortex defined by long-range viral tracing of single neurons. *Nature* **472**, 217–220 (2011).
55. Hirata, T. & Fujisawa, H. Environmental control of collateral branching and target invasion of mitral cell axons during development. *J. Neurobiol.* **38**, 93–104 (1999).
56. Walz, A., Omura, M. & Mombaerts, P. Development and topography of the lateral olfactory tract in the mouse: imaging by genetically encoded and injected fluorescent markers. *J. Neurobiol.* **66**, 835–846 (2006).
57. Hong, W., Kim, D. W. & Anderson, D. J. Antagonistic control of social versus repetitive self-grooming behaviors by separable amygdala neuronal subsets. *Cell* **158**, 1348–1361 (2014).
58. Choi, G. B. *et al.* Lhx6 delineates a pathway mediating innate reproductive behaviors from the amygdala to the hypothalamus. *Neuron* **46**, 647–660 (2005).
59. Stowers, L. & Marton, T. F. What is a pheromone? Mammalian pheromones reconsidered. *Neuron* **46**, 699–702 (2005).
60. Niimura, Y. On the origin and evolution of vertebrate olfactory receptor genes: comparative genome analysis among 23 chordate species. *Genome Biol. Evol.* **1**, 34–44 (2009).
61. Meisami, E. & Bhatnagar, K. P. Structure and diversity in mammalian accessory olfactory bulb. *Microsc. Res. Tech.* **43**, 476–499 (1998).
62. Meredith, M. Human vomeronasal organ function: a critical review of best and worst cases. *Chem. Senses* **26**, 433–445 (2001).
63. Kaneko-Goto, T. *et al.* Goofy coordinates the acuity of olfactory signaling. *J. Neurosci.* **33**, 12987–12996. 12996a (2013).
64. Nagai, Y., Sano, H. & Yokoi, M. Transgenic expression of Cre recombinase in mitral/tufted cells of the olfactory bulb. *Genesis* **43**, 12–16 (2005).
65. Kawashima, T. *et al.* Functional labeling of neurons and their projections using the synthetic activity-dependent promoter E-SARE. *Nat. Methods* **10**, 889–895 (2013).
66. Tsuboi, A. *et al.* Olfactory neurons expressing closely linked and homologous odorant receptor genes tend to project their axons to neighboring glomeruli on the olfactory bulb. *J. Neurosci.* **19**, 8409–8418 (1999).
67. Paxinos, G. & Franklin, K. in *The Mouse Brain in Stereotaxic Coordinates* 4th edn (Academic Press, 2012).
68. Schambra, U. *Prenatal Mouse Brain Atlas* (Springer, 2008).
69. Biffo, S., Verdun di Cantogno, L. & Fasolo, A. Double labeling with non-isotopic *in situ* hybridization and BrdU immunohistochemistry: calmodulin (CaM) mRNA expression in post-mitotic neurons of the olfactory system. *J. Histochem. Cytochem.* **40**, 535–540 (1992).

Acknowledgements

We thank Y. Yoshihara for Goofy-Cre mouse, T. Williams for AP2 ϵ -Cre mouse, E. Callaway for RV and TVA vectors, E. Block and H. Matsunami for MTMT. We are grateful to

L. Luo, A.J. Otsuka and members of our laboratory for valuable comments and discussion. K.I. was a pre-doctoral fellow of the Japan Society for the Promotion of Science, and H.N. was supported by Urakami Foundation. This work was supported by Grants in Aid from the Ministry of Education, Culture, Sports, Science and Technology (MEXT) of Japan (T.K., H.N., H.T., H.B. and H.N.), and by the JST-PRESTO (H.T.) and AMED-CREST (H.B.) programmes. H.S. is funded by the Specially Promoted Research Grants from MEXT of Japan, and F.I. by the NIH Grant, RO3-DC011134. All recombinant DNA and animal experiments were performed in accordance with the regulations and guidelines of the Universities, and approved by the institutional review committees of Graduate School of Medicine and Graduate School of Science, University of Tokyo; School of Medical Science, University of Fukui; and School of Veterinary Medicine, Azabu University.

Author contributions

This research was conceived by K.I., H.T., H.N. and H.S. K.I. performed most of the experiments. *In utero* electroporation experiments were done by F.I. H.O. purified AAV and RV. K.I. and R.K. performed virus injection, and H.B. supervised the virus studies. T.K. oversaw the behavioural analysis. The manuscript was prepared by K.I., H.T., H.N. and H.S.

Additional information

Supplementary Information accompanies this paper at <http://www.nature.com/naturecommunications>

Competing interests: The authors declare no competing financial interests.

Reprints and permission information is available online at <http://npg.nature.com/reprintsandpermissions/>

How to cite this article: Inokuchi, K. *et al.* *Nrp2* is sufficient to instruct circuit formation of mitral-cells to mediate odour-induced attractive social responses. *Nat. Commun.* **8**, 15977 doi: 10.1038/ncomms15977 (2017).

Publisher's note: Springer Nature remains neutral with regard to jurisdictional claims in published maps and institutional affiliations.



Open Access This article is licensed under a Creative Commons Attribution 4.0 International License, which permits use, sharing, adaptation, distribution and reproduction in any medium or format, as long as you give appropriate credit to the original author(s) and the source, provide a link to the Creative Commons license, and indicate if changes were made. The images or other third party material in this article are included in the article's Creative Commons license, unless indicated otherwise in a credit line to the material. If material is not included in the article's Creative Commons license and your intended use is not permitted by statutory regulation or exceeds the permitted use, you will need to obtain permission directly from the copyright holder. To view a copy of this license, visit <http://creativecommons.org/licenses/by/4.0/>

© The Author(s) 2017